

# Study of the Linkage Isomerization $[\text{Co}(\text{NH}_3)_5\text{NO}_2]\text{Br}_2 \rightleftharpoons [\text{Co}(\text{NH}_3)_5\text{ONO}]\text{Br}_2$ in the Solid State by X-ray Powder Diffraction

Norberto Masciocchi,<sup>\*1a</sup> Alexander Kolyshev,<sup>1b</sup> Victor Dulepov,<sup>1b</sup> Elena Boldyreva,<sup>\*1b</sup> and Angelo Sironi<sup>\*1a</sup>

Istituto di Chimica Strutturistica Inorganica, via Venezian 21, Università di Milano, I-20133 Milano, Italy, and Institute for Solid State Chemistry, Russian Academy of Sciences, Derzhavina 18, Novosibirsk 630091, Russia, and Division of Solid State Chemistry, Novosibirsk State University, Pirogova 2, Novosibirsk 630090, Russia

Received September 14, 1993<sup>o</sup>

The solid-state linkage isomerization  $[\text{Co}(\text{NH}_3)_5\text{NO}_2]\text{Br}_2 \rightleftharpoons [\text{Co}(\text{NH}_3)_5\text{ONO}]\text{Br}_2$  was studied, at room temperature, using the X-ray powder diffraction technique. The structure of the photochemically synthesized  $[\text{Co}(\text{NH}_3)_5\text{ONO}]\text{Br}_2$  was solved in the orthorhombic space group  $Cmcm$ , with  $a = 10.8011(7)$  Å,  $b = 8.9692(6)$  Å,  $c = 10.6090(6)$  Å, and  $Z = 4$ , and refined by the Rietveld method, down to  $R_{\text{profile}} = 0.119$ , for 4000 data points collected in the  $10\text{--}90^\circ$  ( $2\theta$ ) range. The changes in the lattice parameters and the structural evolution in the course of the  $\text{ONO} \Rightarrow \text{NO}_2$  linkage isomerization showed the intramolecular nature of the isomerization, with the powders remaining a monophasic system at any time.

## Introduction

Solid-state linkage nitro–nitrito isomerization in  $\text{Co}(\text{III})$ –ammine complexes has been attracting the attention of chemists since the end of the last century, when these compounds were first synthesized by Jørgensen. One of the reasons for this great interest is that the isomerization proceeds intramolecularly not only in solution but also in the solid state. Therefore, the study of the structural aspects of the reaction is important for understanding the interrelation between “intra”- and “inter”-molecular in solid-state reactions, namely, the relationship between an “intramolecular” transformation (linkage isomerization) and the distortion of crystal structure (i.e. change in the “intermolecular” juxtapositions), induced by this intramolecular reorganization.<sup>2</sup>

It has been known from the times of Jørgensen that ONO isomers not only can be synthesized by solution reactions but also are formed when irradiating the corresponding solid  $\text{NO}_2$  isomers. Grenthe and Nordin have noticed that the powder diffraction patterns of  $[\text{Co}(\text{NH}_3)_5\text{ONO}]\text{Cl}_2$ , precipitated from aqueous solutions, and synthesized photochemically, differ.<sup>3</sup> This indicates that the solid-state nitro–nitrito isomerization produces another polymorph of nitrito–chloride as compared with its crystallization from aqueous solution. Later, the same was also shown to be true for other complexes of the series  $[\text{Co}(\text{NH}_3)_5\text{ONO}]\text{X}_2$  ( $\text{X} = \text{Br}, \text{I}$ ).<sup>4</sup> One could expect the structures of the photochemically synthesized polymorphs to “inherit” the main structural framework of the parent nitro isomers, and, at the same time, to “depict” the interactions in the crystals during the nitro–nitrito isomerization. Therefore, a study of the structures of the photochemically synthesized ONO isomers is of particular interest.

One meets with difficulties when applying single-crystal techniques to study the structures of the polymorphs of the nitrito isomers, synthesized photochemically in the solid state, since the crystals are fragmented as a result of mechanical stress, generated during the reaction.<sup>5</sup> Thus, e.g., a recent attempt to use single-crystal techniques to study the structure of photochemically

synthesized  $[\text{Co}(\text{NH}_3)_5\text{ONO}]\text{Cl}_2$  was not successful.<sup>6</sup> Because of the crystal damage suffered by their sample in the course of irradiation and the consequent broadening of the diffraction peaks, the authors of ref 6 were forced to limit their study by a crystal containing only 15% of the –ONO isomer. At the same time, powder diffraction techniques made it possible<sup>7</sup> not only to measure the lattice parameters for a number of photochemically synthesized nitrito isomers  $[\text{Co}(\text{NH}_3)_5\text{ONO}]\text{XY}$  ( $\text{XY} = \text{Cl}_2, \text{Br}_2, \text{I}_2, \text{Cl}(\text{NO}_3), (\text{NO}_3)_2$ ) but also to follow the continuous distortion of the crystal lattice during the reverse nitrito–nitro isomerization.

The study of ref 7 has shown that in the course of nitro–nitrito linkage isomerization,  $[\text{Co}(\text{NH}_3)_5\text{NO}_2]\text{XY} \rightarrow [\text{Co}(\text{NH}_3)_5\text{ONO}]\text{XY}$ , the crystal system either remains unchanged ( $\text{XY} = \text{Cl}(\text{NO}_3), (\text{NO}_3)_2, \text{I}_2$ ) or becomes more symmetric ( $\text{XY} = \text{Cl}_2, \text{Br}_2$ ). The structures of nitro complexes<sup>6,8</sup> are known to be determined by optimum close packing of complex cations.<sup>9</sup> From analysis of the symmetry of the cation sublattice in the starting nitro structures, of the changes of the lattice parameters in the course of linkage nitro–nitrito isomerization<sup>7</sup> and of the possible changes of the symmetry resulting from these changes in lattice parameters,<sup>10</sup> it would seem that the space groups of the photochemically synthesized  $[\text{Co}(\text{NH}_3)_5\text{ONO}]\text{XY}$  ( $\text{XY} = \text{Cl}(\text{NO}_3), (\text{NO}_3)_2, \text{I}_2$ ) must be the same as the space groups of the starting  $\text{NO}_2$  isomers ( $Pna2_1, 14mm$ , and  $Pnam$ , respectively) and that the space group changes from  $C2/c$  to  $Cmcm$  in the case of nitro–nitrito isomerization in  $[\text{Co}(\text{NH}_3)_5\text{NO}_2]\text{Br}_2$  and  $[\text{Co}(\text{NH}_3)_5\text{NO}_2]\text{Cl}_2$ . The indexes  $hkl$  for observed and absent reflections did not contradict this hypothesis, but to test it directly a full profile analysis of X-ray powder diffraction data was required. It was natural to start with the bromide, since, on the one hand, the

<sup>o</sup> Abstract published in *Advance ACS Abstracts*, April 15, 1994.

- (1) (a) Università di Milano. (b) Institute of Solid State Chemistry, Russian Academy of Sciences, and Novosibirsk State University.
- (2) Boldyreva, E. *Izv. Sib. Otd. Akad. Nauk SSSR, Ser. Khim. Nauk* 1982, 5, 18. Boldyreva, E. *Mol. Cryst. Liq. Cryst. Inc. Nonlin. Opt.*, in press.
- (3) Grenthe, I.; Nordin, E. *Inorg. Chem.* 1979, 18, 1869.
- (4) Boldyreva, E.; Dulepov, V.; Podberezhskaya, N.; Burleva, L. Manuscript in preparation.

- (5) Boldyreva, E.; Sidel'nikov, A.; Chupakhin, A.; Lyakhov, N.; Boldyrev, V. *Dokl. Akad. Nauk SSSR* 1984, 277, 893.
- (6) Kubota, M.; Ohba, S.; *Acta Crystallogr.* 1992, B48, 627.
- (7) Boldyreva, E.; Virovets, A.; Burleva, L.; Dulepov, V.; Podberezhskaya, N. V. *Russ. J. Struct. Chem., Russ. Ed.* 1993, 34, 128.
- (8) (a) Boertin, O. *Acta Chem. Scand.* 1968, 22, 2890. (b) Cotton, F. A.; Edwards, W. *Acta Crystallogr.* 1968, B24, 474. (c) Podberezhskaya, N.; Virovets, A.; Boldyreva, E. *Russ. J. Struct. Chem.* 1991, 32, 693. (d) Virovets, A.; Podberezhskaya, N.; Boldyreva, E.; Burleva, L.; Gromilov, S. *Russ. J. Struct. Chem., Russ. Ed.* 1992, 33, 146. (e) Virovets, A. V.; Boldyreva, E. V.; Dulepov, V. E.; Burleva, L. P.; Podberezhskaya, N. V. *Russ. J. Struct. Chem., Russ. Ed.* 1994, 35, 100.
- (9) Podberezhskaya, N.; Yudanov, T.; Magarill, S.; Ipatova, E.; Romanenko, G.; Pervuchina, N.; Borisov, S. *Russ. J. Struct. Chem.* 1991, 32, 894.
- (10) Kolyshev, A. SYMMETRY, a computer program for the analysis of real and pseudosymmetry of various patterns. Novosibirsk, Russia, 1992.

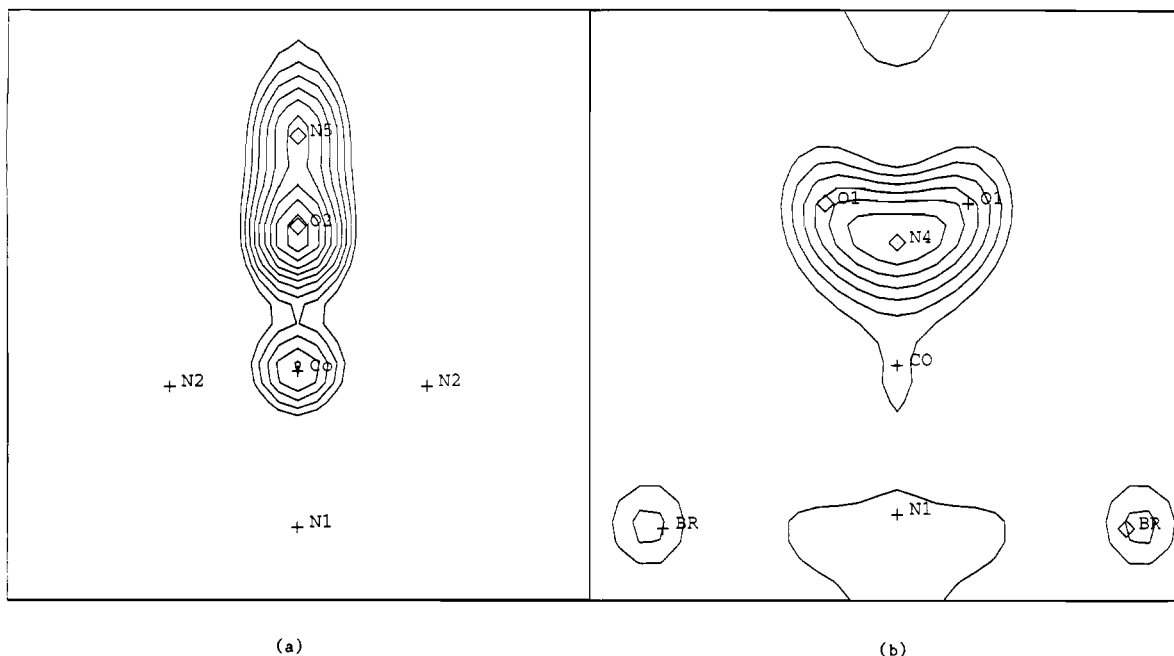


**Figure 1.** (a) Plot of the difference Fourier map after partial refinement of the nitrito phase, the ONO group being omitted from the atom list. Vertical axis is *b*. At this stage, profile agreement factors were  $R = 0.24$  and  $R_w = 0.33$ . Minimum contour level was  $1.20 \text{ e}/\text{\AA}^3$ ; contour interval was  $0.30 \text{ e}/\text{\AA}^3$ . (b) Similar plot for the nitro phase, obtained by omitting the  $\text{NO}_2$  group from the refinement.  $R = 0.19$  and  $R_w = 0.27$ . The section containing the nitro group is shown; again, the vertical axis is *b*. Minimum contour level was  $0.60 \text{ e}/\text{\AA}^3$ ; contour interval was  $0.30 \text{ e}/\text{\AA}^3$ .

crystal system is changed in the course of the isomerization in this compound, which makes the system more interesting, and, on the other hand, in contrast to chloride, all three lattice parameters (*a*, *b*, *c*) in the ONO isomer were measured to be different,<sup>7</sup> so that there seemed to be no pseudosymmetry, resulting from the occasional coincidence of the values of two lattice parameters in the structure, as in the chloride.

The present paper reports on the results of a full profile analysis of X-ray powder diffraction data (XRPD) on  $[\text{Co}(\text{NH}_3)_5\text{ONO}]\text{Br}_2$ , photochemically synthesized in the solid state, and contains (i) solution and refinement of the structure of this polymorph of  $[\text{Co}(\text{NH}_3)_5\text{ONO}]\text{Br}_2$  and (ii) a detailed study of the structural evolution during the reverse solid state  $[\text{Co}(\text{NH}_3)_5\text{ONO}]\text{Br}_2 \rightarrow [\text{Co}(\text{NH}_3)_5\text{NO}_2]\text{Br}_2$  isomerization.

It is worthy noting that, despite a qualitative interpretation of the ONO/ $\text{NO}_2$  isomerization of the chlorine salt from XRPD data was given by Grenthe and Nordin 15 years ago,<sup>3</sup> it was not until recently that digitized powder diffraction data could be suitably handled for structure determination and refinement; their recent use in coordination chemistry has indeed proved to be extremely useful, whenever single crystals could not be prepared.<sup>11</sup>

### Experimental Section

$[\text{Co}(\text{NH}_3)_5\text{NO}_2]\text{Br}_2$  was synthesized as described in ref 12. The yellow-orange powders, precipitated from aqueous solution, were sieved through a 37- $\mu\text{m}$  Teflon net. The sample for X-ray powder diffraction was prepared using a side loading technique,<sup>13</sup> to avoid preferential orientations of the particles. The loosely packed powder sample, about 1 mm thick, was then placed in an horizontal scan Rigaku D III/MAX powder diffractometer, equipped with Soller slits and a graphite monochromator in the diffracted beam. A scintillation Na(Tl)I counter and pulse height discrimination (PHA) were used for measuring the scattered intensities (Cu  $K\alpha$  radiation,  $\lambda = 1.5418 \text{ \AA}$ ). The generator was operated at 40 kV

and 40 mA; slits used: DS,  $1.0^\circ$ ; AS,  $1.0^\circ$ ; and RS,  $0.3^\circ$ . A long overnight run was performed, in the  $10\text{--}110^\circ$  ( $2\theta$ ) range, in the step scan mode, with  $\Delta 2\theta = 0.02^\circ$  and  $t = 10 \text{ s}$ .

At this point, the sample was fully irradiated with direct sunlight for 3 h at  $T = 10^\circ\text{C}$ ,<sup>14</sup> after which a series of XRPD measurements of the red powders was initiated, typically in the  $10\text{--}90^\circ$  ( $2\theta$ ) range with  $\Delta 2\theta = 0.02^\circ$  and  $t = 1 \text{ s}$ . Scan conditions: 40 kV, 40 mA; DS,  $1.0^\circ$ ; AS,  $1.0^\circ$ ; RS,  $0.30^\circ$ . The completeness of the  $\text{NO}_2 \rightarrow \text{ONO}$  isomerization was controlled by XRPD, IR and optical reflectance spectra. In order to follow the reverse ONO- $\text{NO}_2$  solid-state isomerization, 32 data sets have been continuously collected (each spectrum lasting about 2.5 h); in the final runs the changes in the measured patterns were very small. All measurements were performed at room temperature.

The GSAS<sup>15</sup> package of structural solution and refinement programs was used throughout all the XRPD data analyses. Full refinements were performed on the 100%  $\text{NO}_2$  and the 100% ONO transformed data. The background level was modeled by a six-term cosine fourier series, while an asymmetrical Voigt function best accounted for the profile shape. The angular dependence of the peak widths was modelled using the standard Caglioti curve<sup>16</sup> for the Gaussian component, and Hastings and Cox formulas<sup>17</sup> for the Lorentzian fraction. A preferred orientation correction term<sup>18</sup> was introduced in the last stages of the refinement but proved to be unnecessary, as randomization of the particle orientation by the sample preparation technique was successful. All atoms were refined with isotropic thermal factors, and nitrogen and oxygen atoms were constrained to possess identical  $B^2$ 's, twice as high as those of the cobalt atoms to which they are attached; on freeing all thermal parameters, an unlikely spread of values was obtained, as commonly found in XRPD refinements. In order to stabilize the convergence of the nonlinear least-squares, soft restraints on the equatorial Co-N bond distances were introduced [ $\text{Co-N}_{\text{eq}} 2.00(2) \text{ \AA}$ ]. The contribution of the hydrogen atoms to the scattered intensity was neglected. Scattering factors (real and imaginary terms) were taken from the internal library of GSAS.

Refinement of the nitrito phase was performed in the *Cmcm* space group (*vide infra*), initially omitting the atoms of the ONO fragment. Difference Fourier maps showed (see Figure 1a) the location of two peaks, of approximate height of 4 and  $3 \text{ e}/\text{\AA}^3$ , later refined as O and N

(11) Lightfoot, P.; Glidewell, C.; Bruce, P. G. *J. Mater. Chem.* **1992**, *2*, 361. Masciocchi, N.; Moret, M.; Cairati, P.; Ragaini, F.; Sironi, A. *J. Chem. Soc., Dalton Trans.* **1993**, 471. Masciocchi, N.; Cairati, P.; Ragaini, F.; Sironi, A. *Organometallics* **1993**, *21*, 4499.  
 (12) *Gmelins Handbuch der anorganische Chemie, Kobalt (SN 58)*; Springer Verlag: Berlin, 1930; Teil B, S.136.  
 (13) McMurdie, H. F.; Morris, M.; Evans, E.; Paretzkin, B.; Wong-Ng, W. *Powder Diffraction* **1986**, *1*, 40.

(14) The use of a UV lamp was found to be much less effective.  
 (15) Larson, A. C.; Von Dreele, R. B. LANSCE, MS-H805. Los Alamos National Laboratory, Los Alamos, NM, 1990.  
 (16) Caglioti, G.; Paoletti, A.; Ricci, F. P. *Nucl. Instrum.* **1958**, *3*, 223.  
 (17) Thompson, P.; Cox, D. E.; Hastings, J. B. *J. Appl. Crystallogr.* **1987**, *20*, 79.  
 (18) Dollase, W. A. *J. Appl. Crystallogr.* **1986**, *19*, 267; March, A.; *Z. Kristallogr.* **1932**, *81*, 285.

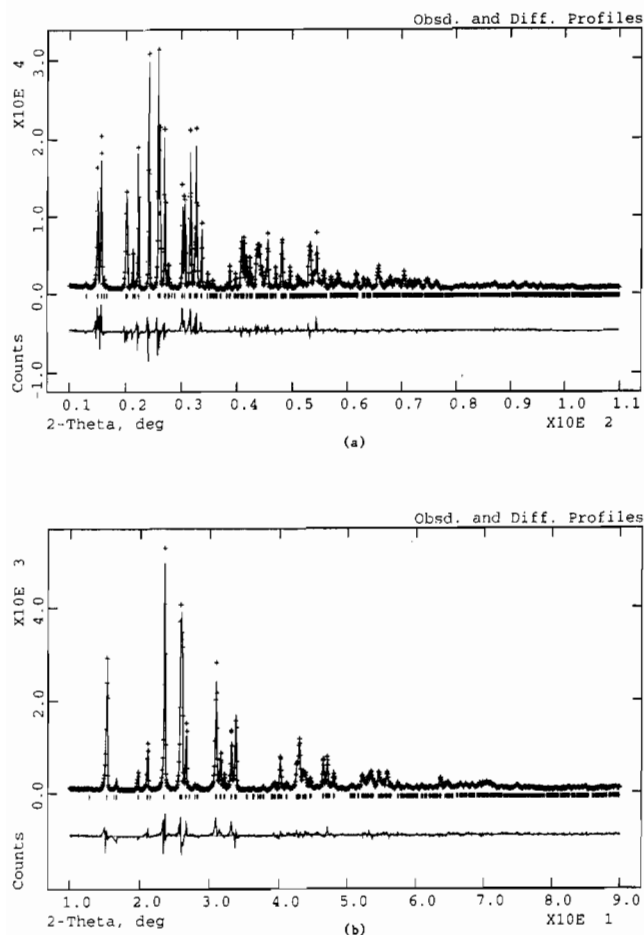


**Figure 2.** Plots of observed and calculated powder diffraction patterns for  $[\text{Co}(\text{NH}_3)_5\text{NO}_2]\text{Br}_2$  (a) and  $[\text{Co}(\text{NH}_3)_5\text{ONO}]\text{Br}_2$  (b). Difference plot is given at the bottom.

atoms, on the 2-fold axis, while no localized electron density higher than  $0.35 \text{ e}/\text{\AA}^3$  could ever be detected for the second oxygen atom, which was then assumed to be disordered over four ( $mm2$  symmetry related) positions about the  $b$  axis<sup>19</sup> and its contribution neglected. Because of the unexpected geometry derived for this Co–O–NO link, several attempts to obtain a more common set of geometrical parameters were performed, either by removing selected symmetry elements about the ONO group (and lowering the space group symmetry down to  $Cmc2_1$ ,  $C2/c$ , and  $Cc$ )<sup>20</sup> and/or by forcing a bent Co–O–N coordination and/or a shorter Co–O distance. During all these attempts, agreement factors heavily worsened, and of greater importance, their difference Fourier maps kept on showing the two strong peaks on the axis.

The experimental and observed patterns are shown in parts a and b of Figure 2, for the nitro and nitrito isomers, respectively. All instrumental parameters were treated as reported above for the nitro phase. Final  $R_p$  values were 0.041 and 0.082, for  $[\text{Co}(\text{NH}_3)_5\text{NO}_2]\text{Br}_2$  and  $[\text{Co}(\text{NH}_3)_5\text{ONO}]\text{Br}_2$ , respectively; although the scattering from the samples above  $80^\circ$  in  $2\theta$  seems to be negligible, nevertheless the few visible features are still well reproduced in our computations; in addition, the background and thermal factor determination is certainly better achieved if a substantially large set of data is used.<sup>21</sup>

All collected datasets were analyzed using the ALLHKL program,<sup>22</sup> *i.e.* a whole-pattern profile fitting technique, which, without reference to

any structural model, allows the refinement of, among others, lattice parameters and diffraction peaks widths, the time dependence of which is discussed later. Of the 32 powder spectra recorded during the reverse isomerization, three were also fully analyzed as described above, at intermediate stages of 15, 40, and 65 h after stopping irradiation; their starting models contained a (variable) fraction of the  $\text{NO}_2$  and  $\text{ONO}$  ligands. Refinement of these values allowed us to estimate the changes in the lattice parameters and cell volume as a function of the relative percentage of nitrito and nitro isomers in the sample.

Final fractional atomic coordinates for both end members, the pure nitro and nitrito phases, are collected in Table 1, while a summary of crystal data, of the refined parameters for the five runs fully analyzed by GSAS is reported in Table 2. Table 3 contains the relevant bond distances and angles for the 100%  $\text{NO}_2$  and 100%  $\text{ONO}$  samples.

## Results and Discussion

**Refinement of the Structure of  $[\text{Co}(\text{NH}_3)_5\text{NO}_2]\text{Br}_2$ .** To test if the technique of sample preparation was satisfactory and the programs used were suitable for the solution of structures of this very type of coordination compounds, we carried out a test refinement of the crystal structure of  $[\text{Co}(\text{NH}_3)_5\text{NO}_2]\text{Br}_2$ , previously studied by Cotton *et al.* by single-crystal X-ray diffraction.<sup>8b</sup> Convergence was rapidly reached on our powder data with the model based on Cotton's data (see Tables 1 and 2). Lattice parameters and fractional coordinates were slightly different compared with Cotton's; the resulting bonding parameters, however, were similar (see Table 3). Figure 1b shows a difference Fourier map for  $[\text{Co}(\text{NH}_3)_5\text{NO}_2]\text{Br}_2$ , in which the  $\text{NO}_2$  fragment, initially omitted from the refinement, was clearly located.

The results obtained on the  $\text{NO}_2$  isomer basically showed that the sample was suitable for structural refinement, as it did not show noticeable preferred orientation effects nor evident peak broadening. In addition, the data analysis and the refinement procedures also gave reliable results, indicating that it was then possible to proceed further with the unknown  $\text{ONO}$  structure.

**Crystal Structure of  $[\text{Co}(\text{NH}_3)_5\text{ONO}]\text{Br}_2$ .** The starting model for the orthorhombic  $[\text{Co}(\text{NH}_3)_5\text{ONO}]\text{Br}_2$  phase was based on the symmetry analysis of the possible topotactic transformations leading, with very little changes of the relative absolute location of the atoms,<sup>23</sup> from  $C2/c$  to  $Cmcm$ <sup>10</sup> (*vide supra*). The successful refinement of the nitrito isomer in  $Cmcm$ , confirmed the aforementioned hypothesis (see Experimental Section). An ORTEP drawing of the  $[\text{Co}(\text{NH}_3)_5\text{ONO}]^{2+}$  cation is shown in Figure 3.

As the  $\text{NO}_2$  ligand changes its coordination from nitro to nitrito, the Co– $\text{NH}_3$  bonds in the complex cation  $[\text{Co}(\text{NH}_3)_5\text{ONO}]^{2+}$  seem to be only slightly affected, at least at the level of accuracy allowed by the method; on the contrary, the  $\text{NO}_2$  fragment, which in the starting isomer lies at about  $1.91(2) \text{ \AA}$  from the cobalt atom, in  $[\text{Co}(\text{NH}_3)_5\text{ONO}]\text{Br}_2$  shows a (long) Co–O bond distance of  $2.24(2) \text{ \AA}$ . In view of the lower stability of the nitrito isomer, it is more natural to expect the Co–ONO bond to be significantly longer than the Co– $\text{NO}_2$  bond; *i.e.*, this value is reasonable and is within the limits reported for other related compounds.<sup>24</sup> The value of the O–N bond length ( $1.36(3) \text{ \AA}$ ) is larger than the corresponding values reported in the literature for  $[\text{Cr}(\text{NH}_3)_5\text{ONO}]\text{Cl}_2$ <sup>25</sup> ( $1.19 \text{ \AA}$ ) or for  $[\text{Co}(\text{NH}_3)_5\text{ONO}]\text{Cl}_2$ , crystallized from solution<sup>3</sup> ( $1.24 \text{ \AA}$ ); however, it agrees well with the formal

- (19) After idealization of the hydrogen atom locations, analysis of interatomic contacts in the crystal lattice and semiquantitative potential energy computations performed with SMILE (Eufri, D.; Sironi, A. *J. Mol. Graph.* **1989**, *7*, 165) clearly showed a 4-fold barrier upon rotation of the O–N–O moiety about the Co–O–N axis. With the O–N–O angle and the external N–O bond length set at  $120^\circ$  and  $1.20 \text{ \AA}$ , respectively, the four minima lie about  $x = 0.068$ ,  $y = 0.751$ ,  $z = 0.181$ , and its symmetry related locations.
- (20) The Co, Br and N (ammonia) atoms have been unambiguously located and refined in  $Cmcm$ , and their positions are essentially unchanged on lowering the space group symmetry.
- (21) Post, J. E.; Bish, D. L. *Modern Powder Diffraction; Reviews in Mineralogy* **20**; The Mineralogy Society of America: Washington, DC, 1989.

- (22) Pawley, G. S.; *J. Appl. Crystallogr.* **1981**, *14*, 357.
- (23) *A posteriori*, the average shift of the (eight) bromide anions surrounding the nitro/nitrito Co complexes was found to be  $0.26 \text{ \AA}$ . This is in good agreement with the homogeneous character of the photochemical transformation, the reversibility of the lattice distortion and of the frequency shifts in the i.r. spectra.
- (24) Hitchman, M.; Rowbottom, G. *Coord. Chem. Rev.* **1982**, *42*, 55. Note that in a number of "conventional" single crystal structural studies of nitrito complexes the ONO stereochemistry was determined "manually" from geometric considerations and *not* detected experimentally.
- (25) Nordin, E. *Acta Crystallogr.* **1978**, *B34*, 2285.

**Table 1.** Fractional Atomic Coordinates for [Co(NH<sub>3</sub>)<sub>5</sub>NO<sub>2</sub>]Br<sub>2</sub> (a) and [Co(NH<sub>3</sub>)<sub>5</sub>ONO]Br<sub>2</sub> (b)

atom	isomer a			isomer b		
	x/a	y/b	z/c	x/a	y/b	z/c
Br	0.2072(2)	0.0139(2)	0.0110(2)	0.2137(2)	0.0	0.0
Co	0.0	0.2888(4)	0.25	0.0	0.2831(6)	0.25
N1	0.0	0.0478(16)	0.25	0.0	0.0423(23)	0.25
N2	0.1863(3)	0.2809(13)	0.2498(10)	0.1850(16)	0.2775(20)	0.25
N3	0.0091(9)	0.2939(12)	0.4325(32)	0.0	0.2819(21)	0.4382(2)
N4	0.0	0.5053(23)	0.25			
O1	0.0739(8)	0.5732(9)	0.1865(8)			
O2				0.0	0.5327(20)	0.25
N5				0.0	0.6842(25)	0.25

**Table 2.** Crystal Data and Summary of Refined Parameters for [Co(NH<sub>3</sub>)<sub>5</sub>NO<sub>2</sub>]Br<sub>2</sub> (a) and [Co(NH<sub>3</sub>)<sub>5</sub>ONO]Br<sub>2</sub> (b) and the Three Intermediate Runs (c–e) Mentioned in the Text: at 15 (c), 40 (d), and 65 h (e) After Stopping Irradiation, Respectively

	a	b	c	d	e
fw,amu	349.90	349.90	349.90	349.90	349.90
2θ range	10–110	10–90	10–90	10–90	10–90
N <sub>obs</sub>	5000	4000	4000	4000	4000
N <sub>refl</sub>	1408	500	904	892	884
system	monoclinic	orthorhombic	monoclinic	monoclinic	monoclinic
space group	C2/c	Cmcm	C2/c	C2/c	C2/c
a, Å	10.6913(4)	10.8011(7)	10.7885(17)	10.7452(7)	10.7247(5)
b, Å	8.8429(3)	8.9692(6)	8.9390(13)	8.9048(5)	8.8836(4)
c, Å	10.9830(4)	10.6090(6)	10.7035(16)	10.8463(7)	10.9168(5)
β, deg	94.575(2)	90.00	90.962(7)	93.274(3)	93.890(3)
V, Å <sup>3</sup>	1035.1(1)	1027.8(2)	1032.1(4)	1036.1(2)	1037.7(1)
Z	4	4	4	4	4
ρ <sub>calc</sub> , g cm <sup>-3</sup>	2.245	2.261	2.251	2.243	2.239
μ, cm <sup>-1</sup>	226.8	228.4	227.4	226.6	226.2
λ, Å	1.5418	1.5418	1.5418	1.5418	1.5418
T, °C	22	22	22	22	22
R <sub>profile</sub> <sup>a</sup>	0.087	0.119	0.161	0.112	0.102
R <sub>w,profile</sub>	0.118	0.157	0.198	0.145	0.133
R <sub>expected</sub>	0.024 <sup>b</sup>	0.069	0.068	0.069	0.069
U(Br), 100 × Å <sup>2</sup>	3.25(7)	5.24(12)	5.57(21)	4.94(14)	4.22(12)
U(Co), 100 × Å <sup>2</sup>	1.28(8)	1.62(12)	1.17(2)	1.60(13)	2.26(23)
%(NO <sub>2</sub> )	100.0	0.0	38(4)	67(2)	83(1)

<sup>a</sup>  $R_{\text{profile}} = \sum |y_{i,o} - y_{i,c}| / \sum y_{i,o}$ .  $R_{w,\text{profile}} = [\sum w_i (y_{i,o} - y_{i,c})^2 / \sum w_i y_{i,o}^2]^{1/2}$ .  $R_{\text{expected}} = [(N_{\text{obs}} - N_{\text{var}}) / \sum w_i y_{i,o}^2]^{1/2}$ .  $y_{i,o}$  and  $y_{i,c}$  are the observed and calculated intensities, respectively, and  $w_i$  is a statistical weighting factor, taken as  $1/y_{i,o}$ . <sup>b</sup> This low value reflects mainly the better counting statistics achieved by longer counting times.

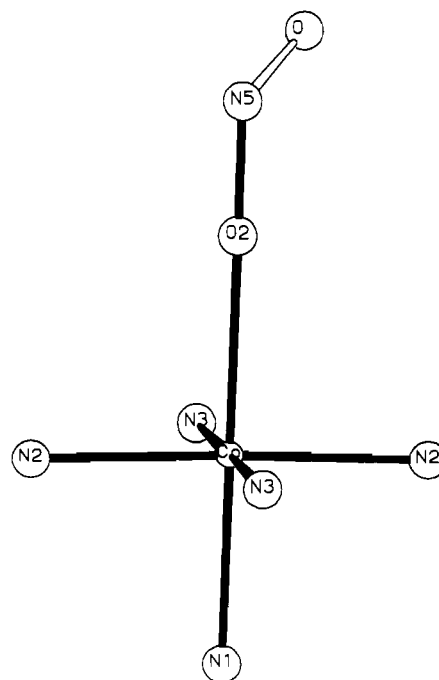
**Table 3.** Relevant Bond Distances (Å) and Angles (deg) for [Co(NH<sub>3</sub>)<sub>5</sub>NO<sub>2</sub>]Br<sub>2</sub> (a) and [Co(NH<sub>3</sub>)<sub>5</sub>ONO]Br<sub>2</sub> (b), and for the Sake of Comparison, Single Crystal Data (Cotton *et al.*<sup>8b</sup>) (c)<sup>a</sup>

	a	b	c
Co–N1	2.13(2)	2.16(2)	1.97(2)
Co–N2	1.99(1)	2.00(1)	1.97(2)
Co–N3	2.00(1)	2.00(1)	1.95(2)
Co–N4	1.91(2)		1.92(2)
N4–O1	1.25(1)		1.23(2)
Co–O2		2.24(2)	
O2–N5		1.36(3)	
N1–Co–N2	87.0(3)	88.6(6)	90.0(4)
N1–Co–N3	91.3(3)	89.7(6)	91.3(4)
N2–Co–N3	91.9(4)	90.0	91.9(6)
N2–Co–N2	176.0(7)	177.1(11)	180.0(6)
N3–Co–N3	177.5(7)	179.4(1)	177.4(6)
N1–Co–N4	180.00		180.00
N2–Co–N4	92.0(3)		90.0(4)
N3–Co–N4	88.7(3)		88.7(4)
N1–Co–O2		180.00	
N2–Co–O2		91.4(6)	
N3–Co–O2		90.3(6)	
Co–N4–O1	119(1)		120.2(3)
O1–N4–O1	122(2)		119.6(6)
Co–O2–N5		180.0	

<sup>a</sup> Due to a mismatch between different tables and figures in ref 8b, these values have been recalculated by us on the basis of the published coordinates.

single bond value observed in other metal nitrito complexes<sup>24</sup> or in organic nitrites such as CH<sub>3</sub>–O–NO.<sup>26</sup>

The value of the Co–O–N angle (180°)<sup>27</sup> differs essentially

**Figure 3.** ORTEP drawing of the [Co(NH<sub>3</sub>)<sub>5</sub>ONO]<sup>2+</sup> ion with the disordered (uncoordinated) oxygen atom set in one of its probable locations.<sup>19</sup>

from the corresponding value of 125.9° reported for [Cr(NH<sub>3</sub>)<sub>5</sub>–ONO]Cl<sub>2</sub>,<sup>25</sup> as well as from the value 131.3° published for

[Co(NH<sub>3</sub>)<sub>5</sub>ONO]Cl<sub>2</sub> crystallized from aqueous solution (disordered structure, with unreliable results).<sup>3</sup> Two other Co(III)–ONO structures, namely *trans*-[Co(en)<sub>2</sub>(NCS)(ONO)](ClO<sub>4</sub>) and *trans*-[Co(en)<sub>2</sub>(NCS)(ONO)](I) (en = ethylene-1,2-diamine) are known in the literature,<sup>28</sup> showing a bent Co–O–N linkage. However, all attempts to change the value of the Co–O–N angle from 180° or to decrease the value of the Co–O and N–O bond lengths (contradicting the location of the O and N atoms as found on the difference Fourier maps)<sup>29</sup> resulted in the essential deterioration of the profile agreement factors.<sup>30</sup>

The disorder of the terminal oxygen atom of the nitrito group might slightly affect the actual locations of the O2 and N5 atoms, casting some doubts on the significance of the observed bond lengths. However, we are quite confident in the overall picture of this unusual ONO geometry, which possibly results from the steric restrictions dictated by the main structural frame of the starting NO<sub>2</sub> isomer.

**Comparison of the Structures of the Nitro and Nitrito Isomeric Forms.** On the basis of the refined cell parameters of the two isomers, one can see that the lattice distortion resulting from the intramolecular change of the NO<sub>2</sub> to ONO coordination is anisotropic. Although the molar volume of [Co(NH<sub>3</sub>)<sub>5</sub>NO<sub>2</sub>]Br<sub>2</sub> is larger than the molar volume of [Co(NH<sub>3</sub>)<sub>5</sub>ONO]Br<sub>2</sub>, formed as a result of the NO<sub>2</sub>–ONO isomerization, there are directions in the crystal, which expand when the NO<sub>2</sub>–ONO isomerization proceeds and the molar volume decreases. The anisotropy of the deformation can be shown most clearly by calculating the strain tensor.<sup>31</sup> It is even easier to visualize the anisotropic deformation of the structure if the strain ellipsoid is plotted with respect to the crystallographic axes,<sup>31</sup> as in Figure 4. It is clearly seen that during the NO<sub>2</sub>–ONO isomerization the lattice slightly expands in the direction of the Co–NO<sub>2</sub> bond (axis *b*, coinciding with principal axis 2 of the strain ellipsoid). The directions of major expansion (principal axis 1) and major contraction (principal axis 3) do not coincide with the direction of any crystallographic axis: that of maximal expansion is perpendicular to the plane of the NO<sub>2</sub> group, and the lattice is compressed in the direction close to the perpendicular to the plane bisecting the O–N–O angle. This seems to indicate that in the course of NO<sub>2</sub>–ONO isomerization the NO<sub>2</sub> group leaves the original plane as the coordination of this group to cobalt is changed. The ONO groups are disordered and thus the 2-fold axis is preserved, although the real symmetry of the complex cation decreases. The symmetry of the crystal lattice becomes even higher as the NO<sub>2</sub>–ONO

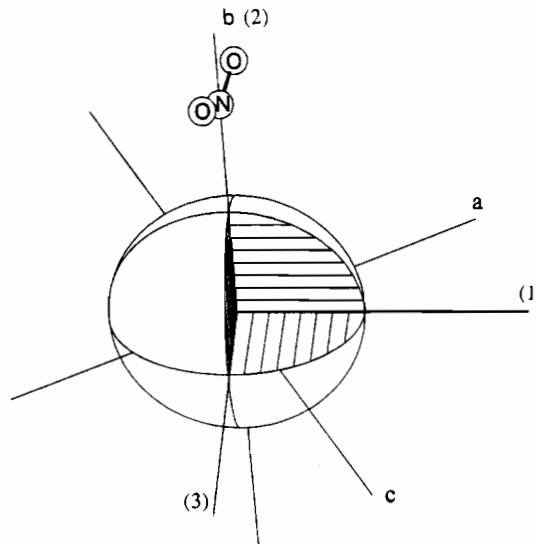


**Figure 4.** Strain ellipsoid for the 100% NO<sub>2</sub>–100% ONO linkage isomerization in [Co(NH<sub>3</sub>)<sub>5</sub>NO<sub>2</sub>]Br<sub>2</sub>, together with the orientation of the NO<sub>2</sub> fragment. It was calculated with the help of the program of Ohashi, published in ref 31. The angles (deg) made by the principal axes (1, 2, and 3) of the ellipsoid with the crystallographic axes (*a*, *b*, and *c*) of the starting NO<sub>2</sub> structure, are as follows: axis 1, 34 (*a*), 90 (*b*), 61 (*c*); axis 2, 90 (*a*), 0 (*b*), 29 (*c*); axis 3, 124 (*a*), 90 (*b*), 90 (*c*). Strain along the principal axes are 0.0351(3); 0.0143(4), and –0.0557(3) (dimensionless), for axes 1, 2, and 3, respectively. Deformation of the plot is exaggerated. The orientations of the strain ellipsoids calculated for the intermediate states during the linkage isomerization (solid solutions of two isomeric forms with different concentrations) slightly differ: the orientation of the axis 2 of the ellipsoid (with respect to the crystallographic axes) remains essentially the same, whereas axes 1 and 3 rotate about 5° as the isomerization proceeds.

isomerization proceeds, since, as a result of the structural distortion due to the recoordination of the NO<sub>2</sub> ligand in the complex cation all the lattice angles become equal to 90° and it is enough to slightly<sup>23</sup> shift the bromine anions (even keeping the positions of the cations constant) to change the symmetry from *C2/c* to *Cmcm*.<sup>10</sup> It should be noted that the refined thermal factors for bromine clearly indicate that either (*i*) they vibrate, in the irradiated form, more than in the starting material, or (*ii*) they suffer from static (or dynamic) disorder, reflecting that of the neighboring ONO moiety.

**Reverse ONO–NO<sub>2</sub> Isomerization at Room Temperature.** The reverse ONO–NO<sub>2</sub> isomerization was followed at room temperature in the dark, without removal of the sample from the diffractometer. In Figure 5 we show a three-dimensional plot of 32 data sets collected continuously (each data collection lasting ca. 2.5 h) after irradiation. The ratio of ONO- and NO<sub>2</sub>-coordinated cations in the sample is found directly from the XRPD refinements of the three selected runs, by refining the site occupancies of the O1 and N5 atoms (with the obvious constraint that their sum is unity) and also estimated from IR and optical reflectance spectroscopy data. In agreement with previously reported results,<sup>7</sup> the solid-state reaction is shown to proceed via the formation of the solid solution of the nitro and nitrito isomers; *i.e.*, at all times during the isomerization, the system remained a monophasic system. It is worth noting that proceeding of nitrito ⇒ nitro linkage isomerisation via formation of solid solutions of one isomeric form in another was reported previously for the ONO–NO<sub>2</sub> isomerization in the crystals of [Co(NH<sub>3</sub>)<sub>5</sub>ONO]Cl<sub>2</sub>, grown from aqueous solutions,<sup>3</sup> in the crystals of *trans*-[Co(en)<sub>2</sub>(NCS)(ONO)](ClO<sub>4</sub>) and *trans*-[Co(en)<sub>2</sub>(NCS)(ONO)](I),<sup>28</sup> and for the NO<sub>2</sub>–ONO isomerization in the [Co(NH<sub>3</sub>)<sub>5</sub>ONO]XY (XY = Cl<sub>2</sub>, Br<sub>2</sub>, I<sub>2</sub>, Cl(NO<sub>3</sub>), (NO<sub>3</sub>)<sub>2</sub>) series.<sup>7</sup> The noticeable lattice distortion resulting from intramolecular isomerization, measured first in ref 7 for a completely isomerized (100%

- (26) Turner, P. H.; Corkill, M. J.; Cox, A. P. *J. Phys. Chem.* **1979**, *83*, 1473.  
 (27) Linear oxygen links are rare, but have been found in a number of oxygen-bridged polynuclear metal complexes such as [(NH<sub>3</sub>)<sub>5</sub>Cr–O–Cr(NH<sub>3</sub>)<sub>5</sub>]Cl<sub>4</sub>·H<sub>2</sub>O (Yevitz, M.; Stanko, J. A. *J. Am. Chem. Soc.* **1971**, *93*, 1514) and in the "ruthenium red" family (Emerson, J.; Clarke, M. J.; Smith, P. M.; Fealey, T.; Earley, J. E.; Silverton, J. V. *Inorg. Chem.* **1971**, *10*, 1943; Ying, W. L.; Sanadi, D. R. *J. Am. Chem. Soc.* **1993**, *115*, 11799 and references therein).  
 (28) Grenthe, I.; Nordin, E. *Inorg. Chem.* **1979**, *18*, 1109.  
 (29) In contrast to the model proposed by Kubota *et al.*,<sup>6</sup> preliminary results obtained by us on the photochemically synthesized crystalline powders of [Co(NH<sub>3</sub>)<sub>5</sub>ONO]Cl<sub>2</sub> also show Fourier maps which can be interpreted only by linearly coordinated –ONO groups.  
 (30) We also tried to use the IR spectra, in the 4000–200-cm<sup>–1</sup> region, in order to characterize the Co–NO<sub>2</sub> and Co–ONO isomers. The spectra confirmed unambiguously the differences in the coordination modes of the nitro ligand in the two isomeric forms; however, it is not so easy to derive information concerning the precise geometry of the Co–ONO form from the spectral data. Model calculations have shown the stretching vibrations of the ONO group (in the 1500–1000-cm<sup>–1</sup> range) to be very little sensitive to the values of the Co–O–NO angle and the Co–O bond length, while vibrations in the far-IR region (400–200-cm<sup>–1</sup>) are not characteristic, *i.e.*, other ligands (NH<sub>3</sub>) contribute significantly to the modes, and this complicates finding a correlation between the Co–ONO geometry and the vibrational frequencies from a comparison with spectral data for related compounds.  
 (31) Hazen, M.; Finger, L. *Comparative Crystal Chemistry. Temperature, Pressure, Composition and the Variation of Crystal Structure*; Wiley: New York, 1982.

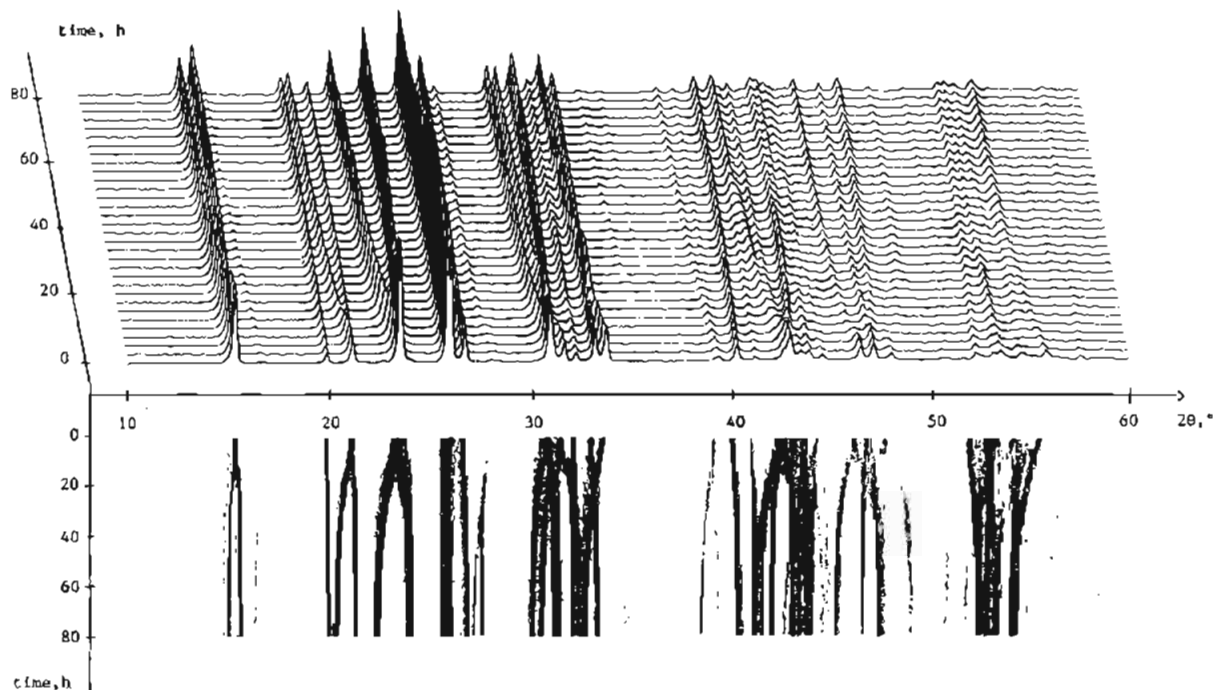


**Figure 5.** Three-dimensional plot (top and side views) of 32 XRPD spectra collected continuously after stopping irradiation (each spectrum took ca. 2.5 h). Note the changes in position and progressive monoclinic splitting of many peaks.

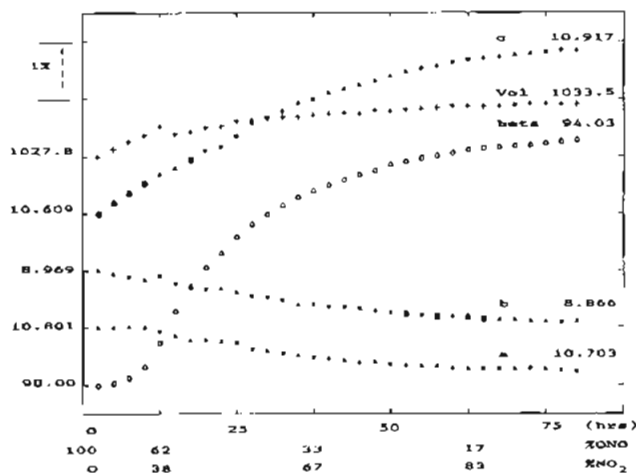


**Figure 6.** Reverse ONO-NO<sub>2</sub> isomerization. Plot of the relative changes of the lattice parameters vs. transformation time. The values reported ([\*] *a, b, c* in Å; [O]  $\beta$  in deg; [+] cell volume in Å<sup>3</sup>) refer to the 100% ONO isomer (left) and to the back-transformed sample after 80 hrs relaxation at room temperature (right, see text). The ratio of the ONO/NO<sub>2</sub> isomeric forms in the sample is also shown.

ONO) complex, is also followed here in detail for the intermediate solid solutions of ONO isomeric form in the NO<sub>2</sub> isomeric form. The changes of unit cell parameters and cell volume vs time are depicted in Figure 6. The changes of the lattice parameters in the course of the isomerization were observed to be continuous, but neither linear with time nor synchronous.<sup>32</sup> The variation of the cell volume, taken vs the percent transformation, as derived by the refinement of the site occupancies of the disordered ONO and NO<sub>2</sub> fragments in the selected intermediate runs (*vide supra*), gives a fairly linear relationship, with a slope of 1.2 Å<sup>3</sup> per 10% transformation. It is also interesting to note that the "asymptotic" value of the cell volume for the thermally converting samples (back to nitro coordination) seems to be slightly higher than that of the freshly prepared starting material, possibly because of

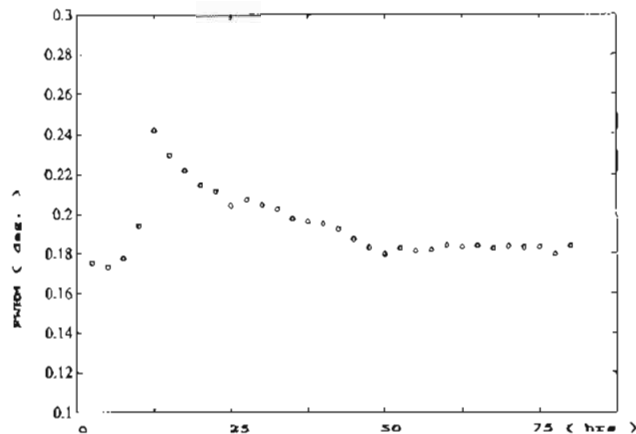


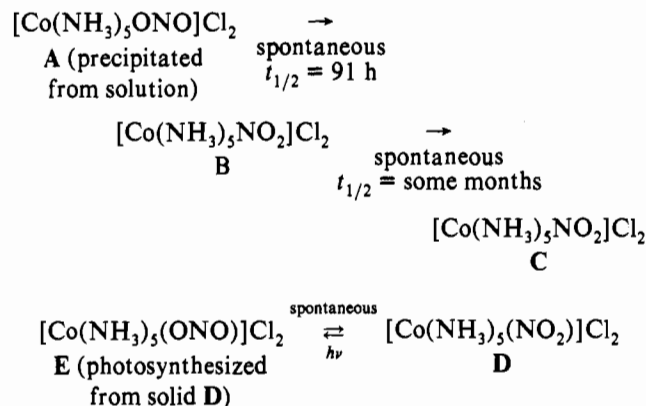
**Figure 7.** Peak widths (pseudo-Voigt fit), computed from the data obtained from whole pattern profile fitting (see Experimental Section) at 15° 2 $\theta$  vs transformation time. Nominal resolution for the present instrumental setup is about 0.14°.

residual strain induced by the photochemical reaction; this was also evidenced by the different angular dependence of the reflection widths in the [Co(NH<sub>3</sub>)<sub>5</sub>NO<sub>2</sub>]Br<sub>2</sub> powders before the irradiation and after the reverse nitrito-nitro isomerization.

Fwhm's (full widths at half-maximum) were measured with time (see Figure 7). The existence of the maximum in Figure 7 and the monophasic nature of the system suggest that the thermal isomerization from ONO to NO<sub>2</sub> coordination is not cooperative but, instead, occurs (stochastically) on the different sites throughout the crystal and that the size of coherent domains is gradually decreased at the beginning of the transformation but is rapidly restored after 15 h. It is worth noting that the maximum of the peak width did not correspond to 50% of the ratio ONO/NO<sub>2</sub> in the sample but was observed at relatively small(er) degrees of the ONO-NO<sub>2</sub> transformation.

The structural aspects of solid-state linkage isomerization were first studied in details by Grenthe and Nordin,<sup>3</sup> who proposed the following reaction scheme for the nitrito/nitro isomerization in the samples of [Co(NH<sub>3</sub>)<sub>5</sub>ONO]Cl<sub>2</sub>, either precipitated from aqueous solution (A) or obtained photochemically in the solid state from the nitro isomer (E):

(32) The cell volume increases linearly within the first 15 h, then abruptly decreases (when the  $\beta$  angle rises dramatically), and later smoothly rises again (see Figure 6).



Powder diffraction revealed the identity of the C and D phases, while A and E, despite of their identical chemical formulas, showed markedly different diffraction spectra. Because of the slow ( $t_{1/2} = 91$  h at 283 K)  $\text{A} \rightarrow \text{B}$  transformation, Grenthe *et al.* were able to collect, and refine, single crystal data from a freshly precipitated sample of A (hence unraveling the nature of the  $\text{A} \rightarrow \text{B} \rightarrow \text{C}$  transformations), but could not characterize the fragmented powder of E. Our work on the bromide analogues is somewhat complementary to the findings of ref 3, in that it shows the nature of the  $\text{E}' \rightleftharpoons \text{D}'$  transformation (primed letters refer to the bromine derivatives).

According to Grenthe and Nordin,<sup>3</sup> an *intramolecular* nitrito/nitro isomerization occurs in the  $\text{A} \rightarrow \text{B}$  reaction, while, on a longer time scale (i.e. some months), *reorientation* of the  $[\text{Co}(\text{NH}_3)_5\text{NO}_2]^{2+}$  complexes in the crystalline lattice is responsible for the  $\text{B} \rightarrow \text{C}$  transformation. At variance, we observe that the *fast* photochemical  $\text{D}' \rightarrow \text{E}'$  transformation does not require any complex reorientation process and that, after stopping irradiation, it is followed by the *slower* reverse isomerization.<sup>33</sup> One can consider the intramolecular linkage isomerization as proceeding within the limits of a "reaction cavity",<sup>34</sup> as it was suggested for the similar reaction in  $[\text{Co}(\text{NH}_3)_5\text{ONO}]\text{XY}$  ( $\text{XY} = \text{Cl}_2, \text{Cl}(\text{NO}_3)^{\text{bc}}$ ). The present study clearly shows that the reaction cavity is not rigid (as it was considered in ref 6) but relaxes as the isomerization proceeds. The change in the coordination of the  $\text{NO}_2$  ligand in the complex cation induces lattice distortion and relative shifts of all the ions.

Obviously, the packing environments of the  $[\text{Co}(\text{NH}_3)_5\text{ONO}]^{2+}$  moieties in A and E are different. Therefore, it is not surprising that the  $-\text{ONO}$  groups may adopt two different conformations in the two polymorphic phases. As a matter of fact, the shape of the cavity occupied by the nitrito group in E' seems to be consistent only with the proposed model, i.e. an almost linear  $\text{Co}-\text{O}-\text{NO}$  coordination, disordered about the  $mm2$  site,<sup>19</sup> possibly in four (symmetry related) positions.

## Conclusions

Full-profile X-ray powder diffraction analysis was shown to be quite powerful in the solution of a number of chemical and

(33) The metric relations between the crystal lattices of the different isomers<sup>7</sup> and our preliminary results on the chlorides suggest that a similar picture must hold also for the  $\text{D} \rightarrow \text{E}$  transformation.

(34) The concept of *reaction cavity* was introduced by Schmidt (Schmidt, G. *Photochemistry of the Solid State*; Interscience: New York, 1967), in order to characterize the crystalline surroundings of a reacting fragment during solid state reactions, and later developed by several authors (see for example: Cohen, M. *Angew. Chem., Int. Ed. Engl.* 1975, 14, 386. Ramamurthy, V.; Venkatesan, K. *Chem. Rev.* 1987, 87, 433. Gavezzotti, A. *Tetrahedron* 1987, 43, 1241. Ohashi, Y.; Yanagi, K.; Kurihara, T.; Sasada, Y.; Ohgo, Y.; *J. Am. Chem. Soc.* 1981, 103, 5805 and references therein).

structural problems, related to the solid state linkage isomerization  $[\text{Co}(\text{NH}_3)_5\text{NO}_2]\text{Br}_2 \rightleftharpoons [\text{Co}(\text{NH}_3)_5\text{ONO}]\text{Br}_2$  (even if compared with single crystal studies of similar reactions in the chloride analogues<sup>3,6</sup>).

(a) It allowed the solution of the structure of the polymorph of  $[\text{Co}(\text{NH}_3)_5\text{ONO}]\text{Br}_2$ , obtained from  $[\text{Co}(\text{NH}_3)_5\text{NO}_2]\text{Br}_2$  in the course of the photoisomerization. The structure of the ONO isomer was shown to be a distorted structure of the starting  $\text{NO}_2$  isomer, with a disordered orientation of the  $-\text{ONO}$  ligand with respect to the crystallographic imposed  $mm2$  symmetry. Whereas the bond lengths in the ONO ligand seem to be within the usual limits, the linear  $\text{Co}-\text{O}-\text{NO}$  linkage appears to be quite unusual and is most probably determined by the restrictions dictated by the main structural frame.

(b) It allowed the continuous distortion of the structure in the course of the reverse nitrito-nitro isomerization to be followed. The lattice distortion resulting from the isomerization was measured as a function of time and of the ratio of the ONO- and  $\text{NO}_2$ -coordinated ligands in the sample. The distortion was shown to be continuous, but anisotropic and not linear with time; apart from a sudden change after about 15 h relaxation, the cell volume was found to depend linearly on the percentage of  $[\text{Co}(\text{NH}_3)_5\text{NO}_2]^{2+}$  in the solid solutions formed during the reaction.

(c) The changes of the complex cations as a result of the intramolecular linkage isomerization were shown to be large enough to induce lattice distortions and shifts of the anions. Anisotropy of the lattice distortions was characterized by plotting of the corresponding strain ellipsoid. The analysis of the van der Waals contacts in the final structure of the nitrito isomer turned out to be helpful to suggest possible locations for the "missing" terminal oxygen atom.<sup>19</sup>

A more detailed analysis of these data and a comparison of the structural deformation in the course of the reaction with that under hydrostatic pressure<sup>35</sup> will hopefully provide essential information concerning the intermolecular interactions in the crystals of nitro and nitritocobalt(III) amines, determining their crystal structures, mechanical properties, and, to no less an extent than intramolecular interactions, the structural mechanism of the solid-state linkage isomerization.

**Acknowledgments.** The authors acknowledge financial support of the study by the Italian Consiglio Nazionale delle Ricerche (Contributo "Altri interventi", AI93.00026.03, for E.B. and Progetto Finalizzato Materiali for N.M. and A.S.), as well as partial support of the work by the program "Universities of Russia" (A.K. and V.D.). The authors are grateful to Dr. L. Burleva for assistance with the synthesis, to Dr. S. Bruni for the optical reflectance spectra and to Dr. S. Lanzavecchia and A. Polyakova for the graphical facilities. E.B. would also like to thank Prof. A. Gavezzotti who made it possible for her to visit the University of Milano for his hospitality and useful and stimulating discussions during her stay. The technical support of Mr. G. Mezza is also acknowledged. Special gratitude is to be expressed to the organizers and sponsors of Erice International School on Crystallography, where E.B. and A.S. were able to meet each other for the first time and to plan the present study.

**Supplementary Material Available:** Detailed lists of crystal data and refined parameters and full lists of bond distances and angles (Tables S1 and S2) and lists of observed and calculated powder pattern data for the 100% nitro and 100% nitrito phases (Tables S3 and S4) (37 pages). Ordering information is given on any current masthead page.

(35) Boldyreva, E.; Ahsbahs, H.; Uchtmann, H. *Ber. Bunsen-Ges. Phys. Chem.*, in the press.